"Physics of Auroral Phenomena", Proc. XLIV Annual Seminar, Apatity, pp. 118-121, 2021

Polar Geophysical Institute

DOI: 10.51981/2588-0039.2021.44.027

THE FEATURES OF PRECIPITATING ELECTRON SPECTRA IN THE RAYED AURORAS

Zh.V. Dashkevich, V.E. Ivanov, B.V. Kozelov

Polar Geophysical Institute, Apatity, Russia

Abstract. The features of auroral electron fluxes, which form rayed structures in auroras, are investigated. The experimental study was the results of triangulation measurements with equipment recording radiation in a wide wavelength range (380–580 nm). It is shown that the spectra of the precipitating electron flux can be approximated by the sum of two electron fluxes having a power-law energy spectrum and a Maxwellian energy distribution.

Introduction

One of the approaches to studying the mechanisms leading to the formation of structured forms of auroras is to study the energy spectra of precipitating electrons. And, while the nature of the energy spectra of auroral electrons, which cause auroras in the form of arcs and stripes, is well known, the spectral characteristics of the electron fluxes that form particular rayed structures have not been practically studied.

Fast spatial dynamics and fluctuations of auroral rayed structures make them difficult to access for direct research on spacecraft. An alternative approach to the study of rayed structures can be ground-based recording of auroras with simultaneous observation from separated points. Such observations make it possible to obtain height profiles of dissipation energy in auroral structures, the nature of which is determined by the form of the energy spectrum of the precipitating electron flux.

Experimental data

Two identical cameras Guppy-1 and Guppy-2 of the MAIN system recorded auroras in Apatity during the 2011-2020 seasons. [*Kozelov et al.*, 2012]. Distance between cameras 4.12 km, angular resolution 0.038 degrees per pixel. The chambers are equipped with the same glass filters to suppress the red part of the optical spectrum. As a result, the spectral bandwidth of the cameras is limited to the range of 380 - 580 nm.

Eight pairs of images of auroral rayed structures forms were selected for processing. These images are presented in Figure 1. The positions of the magnetic zenith in the images are marked with crosses and connected by dotted lines with the corresponding epipolar line. Solid lines mark the images of the auroral ray.

Auroral intensity

The processing of selected pairs of images using epipolar geometry is described in detail in [*Kozelov et al.*, 2021]. At the first stage, the altitude distribution of the integral intensity along the line of sight of the camera was restored. The obtained altitude profiles were recalculated into the altitude distribution of the volume emission rate using the formula:

$$I_v = \frac{I}{L} = \frac{k_{eff} I_c}{\frac{2d}{\sin v}} = \frac{k_{eff} I_c \sin\left(f\sqrt{x^2+y^2}\right)}{2d} \qquad (1)$$

where: I - surface intensity cm^{-2} s^{-1}; I_c - recorded intensity, count s^{-1}; k_{eff} - effective calibration coefficient, cm^{-2} count^{-1}; L - the effective length of the path of the line of sight; d - half-width of the cross-section of the auroral ray, cm; v - the angle between the line of sight and the direction to the magnetic zenith; x, y - position of the pixel on the image relative to the projection of the magnetic zenith; f= 0.038 degrees - angular resolution of cameras.

In formula (1) the effective calibration coefficient k_{eff} determines the relationship between units of the CCD matrix and the value of the surface intensity: $\boldsymbol{I = k_{eff} I_c}$.

When calculating k_{eff}, the spectral components included in the recording range of the device are taken into account. In the general case, it can depend on the parameters of the precipitating electron flux. In [*Kozellov et al.*, 2021], the behavior of k_{eff} was investigated for a wide range of parameters of the precipitating electron flux. It was shown that for Guppy chambers k_{eff} can be considered a constant equal to 9×10^8 cm^{-2} count^{-1}.

The obtained height profiles of the volume emission rates for selected eight cases of auroral rayed structures are shown in Fig. 2. The solid and dashed lines correspond to the profiles reconstructed from the data of the Guppy1 and

Guppy2 cameras. As can be seen, the profiles reconstructed from the data of both cameras coincide both in shape and in absolute values with the error not exceeding 10%.

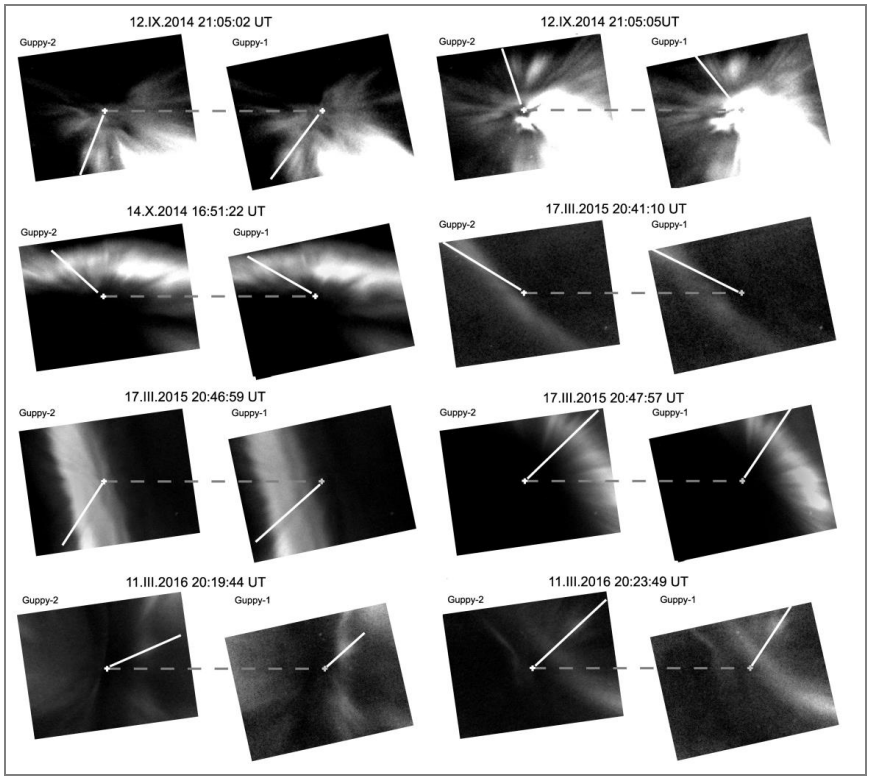

Figure 1. The images recorded by the MAIN cameras for eight cases of rayed forms of auroras.

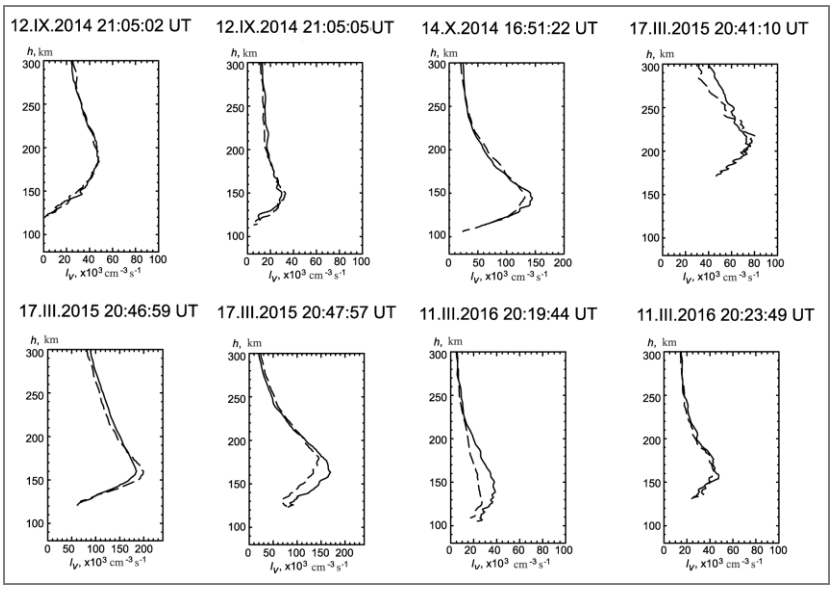

Figure 2. The obtained height profiles of the volume emission rate for eight selected cases of rayed structures.

Estimation of the energy spectra parameters

The energy spectra of flux electric *f(E)* can be found from the equations for the altitude distribution of the energy released in the atmosphere [*Ivanov, Kozelov*, 2001]:

$$W(h) = \rho(h) \int_E \frac{E}{R(E)} \lambda(h,E) f(E) dE, \qquad (2)$$

where: *W(h)* - the deposition energy released at the height h , erg·cm^{-3}s-1; ρ(*h*) - the density of the atmosphere at a height of *h*, g·cm^{-3}; *E* - the energy of an electron, eV; *R(E)* - integral path length, g·cm^{-2}; λ(*h*,*E*) - dimensionless

energy dissipation function describing the fraction of the electron energy released at the height *h*; *f(E)* is the energy spectrum of precipitating electrons, $cm^{-2}\ eV^{-1}s^{-1}$.

The relationship between the volume emission rate and the deposition energy released at the height *h*

$$W(h) = k(h) \cdot I_V(h) \qquad (3)$$

where: *W(h)* is the energy released at height *h*, $I_v(h)$ is the volume emission rate, *k(h)* is the coupling coefficient.

Calculations of *k(h)* carried out in [*Dashkevich et al.*, 2021] showed that *k(h)* has a very weak dependence on both parameters of energy spectrum of precipitating electrons and the concentration of nitric oxide. Figure 3 shows the height dependence of the coefficient *k(h)*. It also shows the standard deviations of this parameter at several heights. It can be seen that the error for the coefficient *k(h)* less that 10%.Thus, the use of this coefficient opens up the possibility of using the observations of auroras by cameras with a wide spectral interval to reconstruct the altitude profiles of energy release.

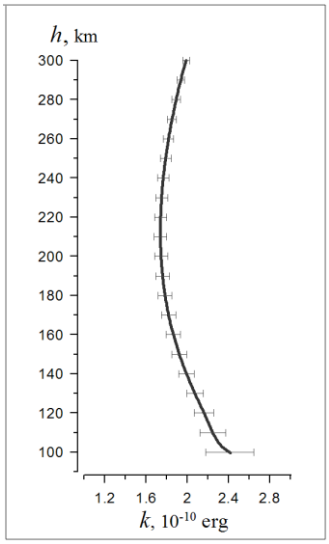

Fig. 3. Height profile k(h)

Using formula (3) the height profiles of volume emission rates $I_v(h)$ were transformed into the height profiles of the deposition energy release *W(h)*. In Figure 4 these profiles are shown in the right panel with a thick line. By solving equation (2) with the energy spectra of precipitating electron fluxes were reconstructed. The obtained energy spectra *f(E)* are shown in Figure 4 on the left panel with a thick line. Two characteristic features can be noted in the behavior of the energy spectrum *f(E)*. In the energy range E =500 ÷1000 eV, a local maximum is observed, while in the energy range E<200 eV the value of the differential electron flux demonstrates a sharp increase with decreasing energy, close to the power-law dependence $E^{-\alpha}$.

This behavior of the *f(E)* curve allows one to approximate the reconstructed energy spectra by the sum of the following functions:

$$F(E) = N_1 E^{-\alpha} + N_2 E_0 \exp(-E/E_0)/E_0^2, \qquad (4)$$

where: E_0 is the characteristic energy.

Figure 4 shows an illustration of the results of approximation of the reconstructed energy spectra by the functional (4) with a thin line. Direct calculations of the deposition energy *W(h)* using the approximation formula show thin line. These calculated deposition energies demonstrate good agreement with the deposition energies reconstructed from the experimental data (thick line).

Figure 5 shows the partial contributions to the deposition energy *W(h)* of electron fluxes with a power-law energy spectrum and Maxwellian energy distribution for selected cases of rayed. It can be seen that at altitudes above 250 km the electron fluxes with a power-law energy distribution forms a significant vertical extent of the deposition energy, and, therefore, the vertical extent of rayed structure intensity. This is a fundamental difference from the altitude distribution of deposition energy in quiet arcs and bands of auroras.

Conclusion

Based on the data of triangulation observations, the features of the energy spectra of precipitating electrons *f(E)*, which form rayed structures in auroras, have been reconstructed and studied. Eight events are considered in the work. It is shown that the behavior of *f(E)* exhibits two characteristic features. In the energy range E =500 ÷1000 eV, local maximum is observed, while in the energy range E<200 eV, a the value of the differential electron flux demonstrates a sharp increase with decreasing energy close to the power-law dependence $E^{-\alpha}$.

It is shown that the obtained distributions *f(E)* are well approximated by the sum of two functions having a power-law character and a Maxwellian energy distribution.

Reference

1. Dashkevich Zh.V., Ivanov V.E., Kozelov B.V. Studying rayed structures in auroras by triangulation methods: 2. Energy spectra of precipitating electrons // Cosmic Research, V.59. P.307-311. 2021. DOI:10.1134/S0010952521050038
2. Ivanov V.E., Kozelov B.V. Transport of electron and proton-hydrogen fluxes in the Earth atmosphere // Apatity. Kola Science Centre. 2001. 260 p.
3. Kozelov B.V., Dashkevich Zh.V., Ivanov V.E. Study rayed structures in auroras by triangulation methods: 1. Height profiles of volume emission rate // Cosmic Research, V.59. P.223-230. 2021. DOI:10.1134/S0010952521040031
4. Kozelov B.V., Pilgaev S.V., Borovkov L.P., and Yurov V.E. Multi-scale auroral observations in Apatity: winter 2010–2011 // Geosci. Instrum. Method. Data Syst. V.1. P.1-6. 2012.

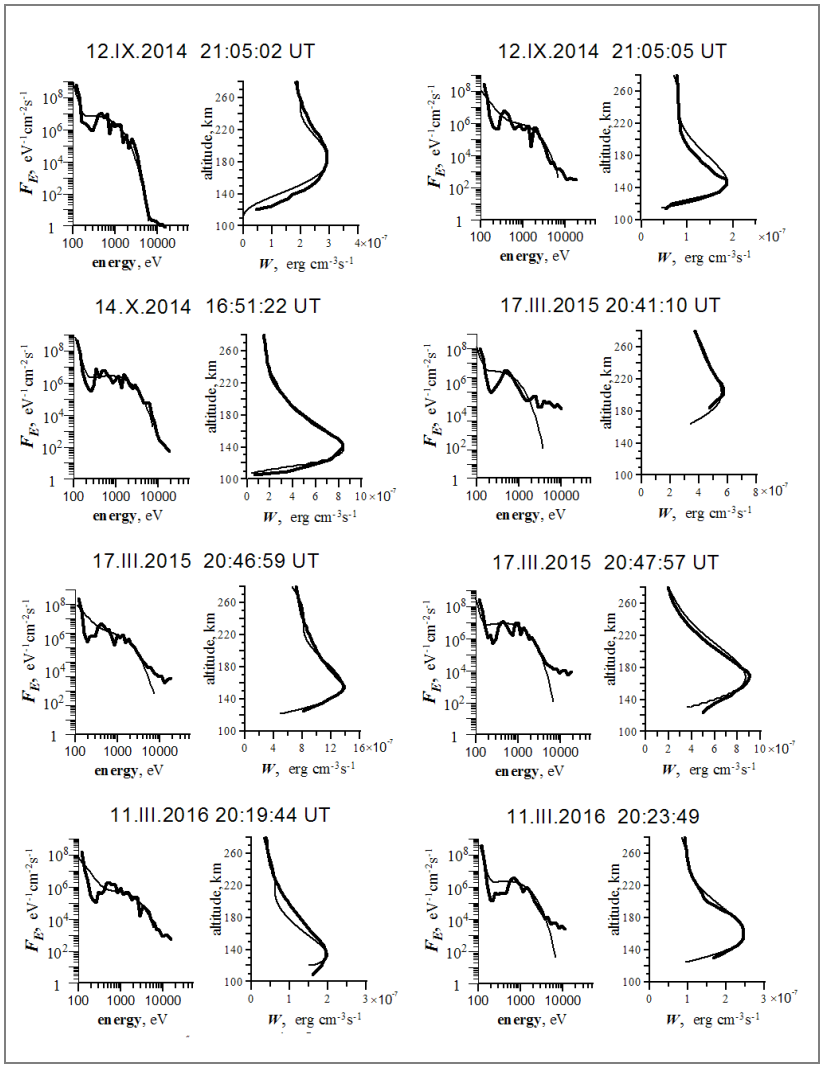

Figure 4. Left panel - reconstructed energy spectra *f(E)* (thick line), approximation of reconstructed energy spectra by the formula (4) (thin line). Right panel - reconstructed height profiles of the deposition energy *W(h)* (thick line); calculated altitude profiles *W(h)* for fluxes described by an approximation formula (4) (thin line).

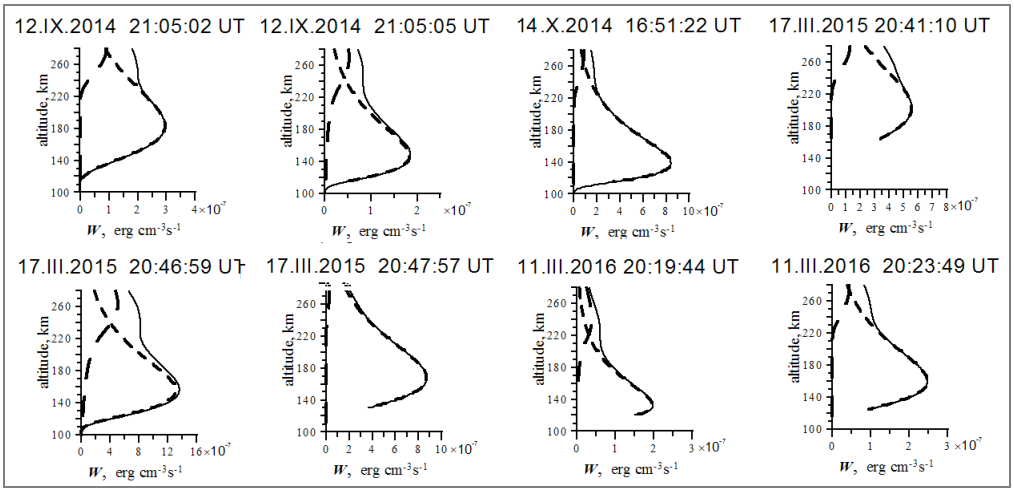

Figure 5. The partial contributions to the height profiles of the deposition energy *W(h)* (solid line) of the electron fluxes with a Maxwellian energy distribution (shot dashed line) and a power-law distribution (long dashed line).